

LETTER TO THE EDITOR

The detection of magnetic chemically peculiar stars using Gaia BP/RP spectra

E. Paunzen¹ and M. Prišegen^{2, 1}

¹ Department of Theoretical Physics and Astrophysics, Faculty of Science, Masaryk University, Kotlářská 2, 611 37 Brno, Czech Republic, e-mail: epaunzen@physics.muni.cz

² Advanced Technologies Research Institute, Faculty of Materials Science and Technology in Trnava, Slovak University of Technology in Bratislava, Bottova 25, 917 24 Trnava, Slovakia

ABSTRACT

Context. The magnetic chemically peculiar (mCP) stars of the upper main sequence are perfectly suited to studying the effects of rotation, diffusion, mass-loss, accretion, and pulsation in the presence of an organized stellar magnetic field. Therefore, many important models can only be tested with this star group.

Aims. In this case study we investigate the possibility of detecting the characteristic 520 nm flux depression of mCP stars using low-resolution BP/RP spectra of the *Gaia* mission. This would enable us to effectively search for these objects in the ever-increasing database.

Methods. We employed the tool of Δa photometry to trace the 520 nm flux depression for 1240 known mCP and 387 normal-type objects including binaries. To this end, we folded the filter curves with the BP/RP spectra and generated the well-established color-color diagram.

Results. It is clearly possible to distinguish mCP stars from normal-type objects. The detection rate is almost 95% for B- and A-type objects. It then drops for cooler-type stars, which is in line with models of the 520 nm flux depression.

Conclusions. The BP/RP spectra are clearly qualified to efficiently search for and detect mCP stars.

Key words. stars: chemically peculiar – stars: magnetic field – stars: statistics – techniques: spectroscopic

1. Introduction

The chemically peculiar (CP) stars with spectral types from early B to early F are traditionally characterized by the presence of certain stellar absorption lines of abnormal strength or weakness that indicate peculiar surface abundances (Preston 1974). Current theories ascribe the observed chemical peculiarities to the interplay between gravitational settling (atomic diffusion) and radiative levitation (Richer et al. 2000). Furthermore, convection, He settling, mass loss, and turbulent mixing can significantly affect the chemical composition of CP stars (Théado et al. 2005).

Many CP stars possess stable and globally organized magnetic fields with strengths of up to several tens of kG (Romanyuk & Kudryavtsev 2008). These stars are often referred to as magnetic chemically peculiar (mCP) stars in the literature. The origin of the magnetic field is still a matter of some controversy (Braithwaite & Spruit 2004). Recently, there was also classical pulsation among mCP stars found (Holdsworth 2021). Therefore, these objects are perfect astrophysical laboratories for investigating the most important phenomena occurring on the upper main sequence in the presence of a stellar magnetic field.

Hümmerich et al. (2020) made use of the 520 nm flux depression, typically for mCP stars, to search for these objects by classifying spectra from the Large Sky Area Multi-Object Fiber Spectroscopic Telescope (LAMOST, Cui et al. 2012). It was shown (Khan & Shulyak 2007) that Fe is the principal contributor to the 520 nm depression for the whole range of effective temperatures (T_{eff}) of mCP stars, while Cr and Si play a role primarily in the low T_{eff} region. However, a strong 520 nm flux

depression was not found for all mCP stars (Kudryavtsev et al. 2006). The reason for this is most probably the individual magnetic field configuration together with the line of sight.

Motivated by the success of Hümmerich et al. (2020), we employed the Δa photometric system which measures the above-mentioned flux depression (Paunzen et al. 2005c; Stigler et al. 2014) to the low-resolution blue photometer and red photometer (BP/RP) spectra of the *Gaia* mission (Carrasco et al. 2021). These spectra cover the wavelength region from 330 to 1050 nm with a resolving power between 25 and 100, depending on the wavelength. The signal-to-noise ratio depends on the apparent magnitude and color of the object. The *Gaia* consortium put a lot of effort into bringing all spectra onto a common flux and pixel (pseudo-wavelength) scale, taking into account variations over the focal plane. Finally, they produced a mean spectrum from all the observations of the same source (Montegriffo et al. 2022). The spectra are available in a continuous representation, with a subset of sources having spectra in a sampled form as well. The *Gaia* DR3 already includes about 219 000 000 mean BP/RP spectra for objects up to the 18th magnitude in *G*.

The spectra are therefore perfectly suited to performing a case study if the known mCP stars can be efficiently detected using the 520 nm flux depression and synthetic Δa magnitudes.

2. Target selection

For the apparent normal stars, we chose all the objects included in the papers by Paunzen et al. (2005b, 2006), who presented an empirical T_{eff} calibration for B- to F-type stars. In total, 387

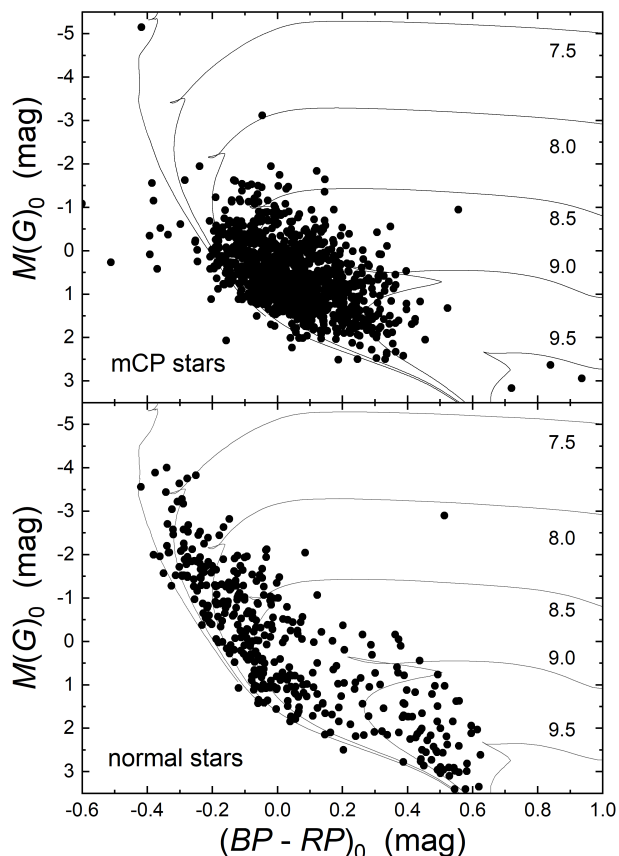


Fig. 1. Diagram of $M(G)_0$ vs $(BP - RP)_0$ for the mCP (upper panel) and normal-type stars (lower panel) together with isochrones from Bressan et al. (2012) for solar metallicity $[Z] = 0.0152$ dex. The two samples overlap.

stars also have an available BP/RP spectrum. We note that this sample also includes binary stars. Among them, 182 objects have a “Dup” flag equal to one and/or a RUWE parameter larger than 1.5, which are both good indicators of binarity (Zavada & Příska 2022).

The mCP stars were chosen from the following references; some stars were listed more than once:

- Paunzen et al. (2005c): We selected all stars with $\Delta a > +20$ mmag from this catalogue of Δa measurements.
- Chojnowski et al. (2019): They published a list of 157 mCP stars with resolved magnetically split lines from the Sloan Digital Sky Survey (SDSS)/Apache Point Observatory Galactic Evolution Experiment (APOGEE) survey.
- Hümmerich et al. (2020): Spectra from the LAMOST Survey showing a 520 nm flux depression were used to find a sample of 1002 mCP stars.

From this large selection, 1240 mCP stars have a BP/RP spectrum. For both samples, we made no cut according to the signal-to-noise ratios of the spectra. To check if both samples are overlapping in the color-magnitude diagram (CMD), we used the photometry and distances from the *Gaia* DR3 (Bailer-Jones et al. 2021; Gaia Collaboration et al. 2022). Furthermore, the reddening values of the individual stars were taken from Paunzen et al. (2005b, 2006); Netopil et al. (2008); Hümmerich et al. (2020). If no value was found, the reddening map of Green et al.

Table 1. Statistics of the detection level for the synthetic Δa values (Figure 2). The numbers for “+” and “−” mean above and below the 95% prediction band of the normality line. The listed ratios should ideally be 100 for the mCP stars and 0 for the normal-type stars.

$(g_1 - y)$	N_{CP-}	N_{CP+}	%	N_{norm-}	N_{norm+}	%
8.0–8.5	0	4	100	2	0	0
8.5–9.0	3	25	89	32	0	0
9.0–9.5	7	132	95	106	0	0
9.5–10.0	12	202	94	85	0	0
10.0–10.5	16	240	94	48	0	0
10.5–11.0	15	247	94	25	0	0
11.0–11.5	23	150	87	29	1	3
11.5–12.0	13	82	86	26	0	0
12.0–12.5	9	36	80	16	1	6
12.5–13.0	10	14	58	7	0	0

(2019) was applied. The individual reddening values were transformed to the *Gaia* filters according to the recommendations by the *Gaia* consortium¹. We note that most stars are in the solar neighborhood ($d < 500$ pc), and therefore the reddening is not significant.

In Fig. 1 the $M(G)_0$ versus $(BP - RP)_0$ diagram is presented for the two samples, together with isochrones from Bressan et al. (2012) for solar metallicity $[Z] = 0.0152$ dex. The normal-type stars (including binaries) cover the whole spectral range and the main sequence very well. No stars can be found below the zero age main sequence, which provides confidence in our method and reddening selection. The mCP stars, except for a few outliers, are located in the same region in the CMD (i.e., in the same astrophysical parameter space).

3. Analysis

To calculate the synthetic magnitudes in the Δa photometric system, we used the approach published in Stigler et al. (2014). We first normalized all spectra to the flux given at 402 nm. Then they were interpolated in the wavelength region from 480 to 580 nm to a one-pixel resolution of 0.1 nm applying a standard polynomial technique. This works perfectly because this wavelength region is very smooth.

For the filter curves, the central wavelengths as published by Maitzen & Seggewiss (1980) were employed: g_1 (501 nm), g_2 (521.5 nm), and y (548.5 nm) with a bandwidth of 13 nm. According to Stigler et al. (2014), this results in the most significant Δa values. The final magnitudes for the three filters are in arbitrary units. It is not straightforward to determine the errors of the magnitudes. Because we did not limit the signal-to-noise ratios (S/N) of the spectra, the source of this error was taken into account. For each spectrum, we took the given S/N and randomly added an error to the individual fluxes. For the lowest S/N, values of about 10, we deduced an error of 1.5%, which does not affect the conclusions and detection limits.

As the last step, we generated the a versus $(g_1 - y)$ diagram for the normal type and mCP stars, which is shown in Figure 2. As can be seen, the normal stars show a distinct band and are clearly separated from the mCP objects. We determined the normality line as in the classical Δa photometric system (i.e., assuming that all stars exhibit the same interstellar reddening; peculiar objects deviate from it by more than 3σ). For the normal-type star sample, it was calculated as

$$a = -2.16(8) + 0.363(8)(g_1 - y) \quad (1)$$

¹ <https://www.cosmos.esa.int/web/gaia/edr3-extinction-law>

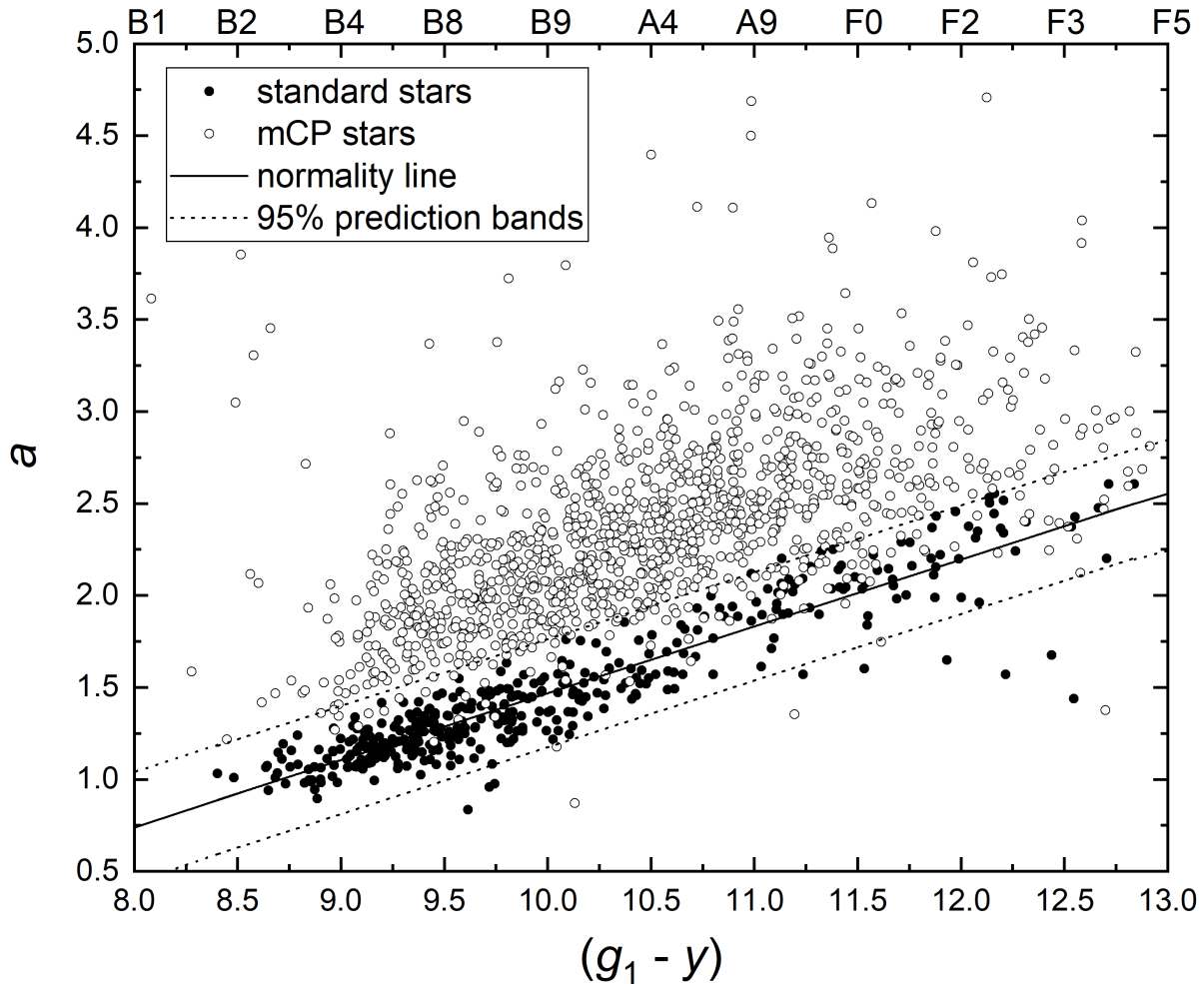


Fig. 2. The a versus $(g_1 - y)$ diagram for the 387 normal type (filled symbols) and 1240 mCP stars (open symbols). The normality line $a = -2.16(8) + 0.363(8)(g_1 - y)$ is defined as in the classical Δa photometric system. The dotted lines are the 95% prediction bands to select mCP stars. We also indicated the approximate spectral types according to the CMD (Figure. 1).

in the units of our synthetic photometric system. The characteristics are similar to the observed normality lines for open clusters (Netopil et al. 2007; Paunzen et al. 2014). The color $(g_1 - y)$ is well correlated with the T_{eff} , especially from late B- to early F-type stars. We split the sample into $(g_1 - y)$ bins and counted how many stars are below (“−”) and above (“+”) the normality line. The latter is the region where the mCP stars are located. In Table 1 the results are presented for both samples. In total, from 387 normal stars, only 2 are located slightly above the prediction band of the region of the mCP objects. From the 1240 mCP stars, 108 (8.7%) are below the upper 95% prediction band. However, the distribution of the latter is homogeneous over the $(g_1 - y)$ range. Most of them are located among cooler-type objects. This effect is already known, as Khan & Shulyak (2006, 2007) showed that the capability of the Δa photometric system drops significantly for stars with T_{eff} lower than 8000 K. This is due to the observational fact that the 520 nm flux depression becomes less prominent compared to the overall line blanketing (Kupka et al. 2004). For the B- and A-type stars we achieved detection rates of almost 95%, which is equivalent to a photometric accuracy of 10 mmag for classical CCD observations (Paunzen et al. 2005c).

4. Conclusions

We showed that, with the help of the low-resolution BP/RP spectra of the *Gaia* mission, it is possible to efficiently search for and detect classical magnetic chemically peculiar (mCP) stars of the upper main sequence. This was done by calculating magnitudes within the Δa photometric system which traces the flux depression at 520 nm typically for this star group. The latter are benchmark objects for studying the effects of rotation, diffusion, mass loss, and pulsation in the presence of an organized local stellar magnetic field.

Using well-known mCP stars and a sample of normal type stars (including about 50% binaries), an almost 95% detection rate for B- and A-type stars was achieved. With our technique it is therefore possible to pre-select the best candidates for further spectroscopic and photometric studies. Querying the different catalogues of the *Gaia* DR3, we found spectral tags indicating approximately 13 million B- and A-type stars up to $G = 17.65$ mag among the published data release. Paunzen et al. (2005a) estimated the lower incidence of all CP stars in the Milky Way of 6% with a published maximum value of at least 16%, respectively. The mCP stars account for about one-third of all CP objects. Therefore, we adopt a mean value of 3% for the considered spectral type range. The ratio of mCP stars that are part of binary systems is still inconclusive (Paunzen 2020).

In total, we estimate $\sim 2 \times 10^5$ mCP stars to be potentially detectable for the discussed accuracy of the presented synthetic $\Delta\alpha$ photometry.

Acknowledgements. This work was supported by the European Regional Development Fund, project No. ITMS2014+: 313011W085. This work presents results from the European Space Agency (ESA) space mission Gaia. Gaia data are being processed by the Gaia Data Processing and Analysis Consortium (DPAC). Funding for the DPAC is provided by national institutions, in particular the institutions participating in the Gaia MultiLateral Agreement (MLA). The Gaia mission website is <https://www.cosmos.esa.int/gaia>. The Gaia archive website is <https://archives.esac.esa.int/gaia>. This research has made use of the SIMBAD database, operated at CDS, Strasbourg, France and of NASA's Astrophysics Data System Bibliographic Services.

References

- Bailer-Jones, C. A. L., Rybizki, J., Fouesneau, M., Demleitner, M., & Andrae, R. 2021, *AJ*, 161, 147
- Braithwaite, J. & Spruit, H. C. 2004, *Nature*, 431, 819
- Bressan, A., Marigo, P., Girardi, L., et al. 2012, *MNRAS*, 427, 127
- Carrasco, J. M., Weiler, M., Jordi, C., et al. 2021, *A&A*, 652, A86
- Chojnowski, S. D., Hubrig, S., Hasselquist, S., et al. 2019, *ApJ*, 873, L5
- Cui, X.-Q., Zhao, Y.-H., Chu, Y.-Q., et al. 2012, *Research in Astronomy and Astrophysics*, 12, 1197
- Gaia Collaboration, Vallenari, A., Brown, A. G. A., et al. 2022, *arXiv e-prints*, *arXiv:2208.00211*
- Green, G. M., Schlafly, E., Zucker, C., Speagle, J. S., & Finkbeiner, D. 2019, *ApJ*, 887, 93
- Holdsworth, D. L. 2021, in *MOBSTER-1 virtual conference: Stellar Variability as a Probe of Magnetic Fields in Massive Stars*, 27
- Hümmerich, S., Paunzen, E., & Bernhard, K. 2020, *A&A*, 640, A40
- Khan, S. A. & Shulyak, D. V. 2006, *A&A*, 448, 1153
- Khan, S. A. & Shulyak, D. V. 2007, *A&A*, 469, 1083
- Kudryavtsev, D. O., Romanyuk, I. I., Elkin, V. G., & Paunzen, E. 2006, *MNRAS*, 372, 1804
- Kupka, F., Paunzen, E., Iliev, I. K., & Maitzen, H. M. 2004, *MNRAS*, 352, 863
- Maitzen, H. M. & Seggewiss, W. 1980, *A&A*, 83, 328
- Montegriffo, P., De Angeli, F., Andrae, R., et al. 2022, *arXiv e-prints*, *arXiv:2206.06205*
- Netopil, M., Paunzen, E., Maitzen, H. M., North, P., & Hubrig, S. 2008, *A&A*, 491, 545
- Netopil, M., Paunzen, E., Maitzen, H. M., et al. 2007, *A&A*, 462, 591
- Paunzen, E. 2020, *Contributions of the Astronomical Observatory Skalnaté Pleso*, 50, 570
- Paunzen, E., Netopil, M., Maitzen, H. M., et al. 2014, *A&A*, 564, A42
- Paunzen, E., Pintado, O. I., Maitzen, H. M., & Claret, A. 2005a, *MNRAS*, 362, 1025
- Paunzen, E., Schnell, A., & Maitzen, H. M. 2005b, *A&A*, 444, 941
- Paunzen, E., Schnell, A., & Maitzen, H. M. 2006, *A&A*, 458, 293
- Paunzen, E., Stütz, C., & Maitzen, H. M. 2005c, *A&A*, 441, 631
- Preston, G. W. 1974, *ARA&A*, 12, 257
- Richer, J., Michaud, G., & Turcotte, S. 2000, *ApJ*, 529, 338
- Romanyuk, I. I. & Kudryavtsev, D. O. 2008, *Astrophysical Bulletin*, 63, 139
- Stigler, C., Maitzen, H. M., Paunzen, E., & Netopil, M. 2014, *A&A*, 562, A65
- Théado, S., Vauclair, S., & Cunha, M. S. 2005, *A&A*, 443, 627
- Zavada, P. & Píška, K. 2022, *AJ*, 163, 33